

C
H
A
P
T
E
R



6

Pluronic mediated silica nanoparticles with chitosan as composite for the dye removal

Chapter-6: Pluronic mediated silica nanoparticles with chitosan as composite for the dye removal

Following to the Chapter 5, In the present chapter work focuses on the use of developed chitosan-modified SiO₂NPs (Ch/ SiO₂NPs) biosorbent for the removal of Congo red (CR) dye from the water for better environmental applications.

6.1: Preparation of Pluronic mediated SiO₂NPs using peanut shell ash (PSA)

The detailed preparation of Pluronic mediated SiO₂NPs used in this present work is given in *Chapter 5* at the *experimental section* under the point **5.2.1**. Briefly, we stirred 350 g of PSA in 0.2 M HCl at 450 rpm for 3 h. The residue was filtered, washed, dried at 95°C, and sieved. The PSA was mixed with NaOH (1:3 ratio) and heated at 100°C for 4 h, followed by refluxing with deionized water for 4 h. After filtration, the sodium silicate solution was collected. Next, 20 mL of 5 wt% Pluronic solution was slowly added to the sodium silicate solution with stirring. The solution was neutralized to pH 7 using 0.1 M sulfuric acid, aged at RT for 3 h, then centrifuged. The SiO₂NPs were collected, washed, and dried at 95°C for 2 h.

6.2: Preparation of Chitosan-modified SiO₂NPs (Ch/SiO₂NPs)

The detailed preparation of chitosan-modified SiO₂NPs (Ch/SiO₂NPs) used in this present work is given in *Chapter 5* at the *experimental section* under the point **5.2.2**. Here, varying amounts of chitosan (0.5, 1.0, 1.5, and 2.0 g) were dissolved in 100 mL of 2% acetic acid. Then, 10 g of Pluronic mediated SiO₂NPs was added and stirred for 24 h to allow homogeneous distribution of chitosan molecules in the SiO₂NPs pores. The mixture was centrifuged, filtered, washed with ultrapure water, and dried in a vacuum oven at 50°C for 6 h to obtain the solid Ch/SiO₂NPs biosorbent.

6.3: Dye removal study

The CR dye removal studies were performed on an initial dye concentration varied from 25 mg/L to 500 mg/L using biosorbent Ch/SiO₂NPs through dye adsorption experiment. The adsorption experiments were carried out batchwise at varied 10°C, 25°C, 30°C, and 50°C temperature. An adsorbent dose of 50 mg Ch/SiO₂NPs were added into the aqueous CR dye solution and stirred at a speed of 150 rpm for varied time durations ranging from 0 to 780 min. The experiments were conducted in triplicate. Analytical curve (shown in Figure 6.1) was developed to find the dye concentration in an aqueous solutions with a known concentration of the CR dye dissolved in water and absorbance was measured using a UV-visible spectrophotometer (UV1900, Shimadzu) at λ_{\max} =498 nm. After treatment with the biosorbent,

Chapter-6: Pluronic mediated silica nanoparticles with chitosan as composite for the dye removal

the dye samples were centrifuged at 1500 rpm, and the absorbance of the supernatant was measured. The percentage of CR dye removal was calculated using Equation 1.

$$\% \text{ Removal} = \frac{(C_i - C_f)}{C_i} \times 100 \text{ ----- (1)}$$

Here, C_i and C_f represent the initial and final CR concentrations, respectively.

The amount of CR adsorption, represented by q_e and q_t (mg/g), was determined by applying equations 2 and 3.

$$q_e = \frac{(C_i - C_e)}{m} \times V \text{----- (2)}$$

$$q_t = \frac{(C_i - C_f)}{m} \times V \text{----- (3)}$$

Here, C_i , C_f , and C_e (mg/L) denote the initial, final, and equilibrium concentrations of CR dye, respectively. The volume of the CR dye solution is denoted by V (L), and m (g) represents the mass of biosorbent. Recyclability experiments were carried out in a manner similar to the adsorption studies. In these tests, the same Ch/SiO₂NPs biosorbent was used multiple times. After each cycle, the dye solution was replaced with a fresh one at a constant concentration, allowing the adsorbent's reusability and performance to be evaluated over successive adsorption cycles.

6.4: Results and discussion

6.4.1: Characterization of Pluronic mediated SiO₂NPs and Chitosan-modified SiO₂NPs (Ch/SiO₂NPs)

The Pluronic mediated SiO₂NPs were synthesized using PSA, followed by surface modification with chitosan, resulting in chitosan-modified SiO₂NPs (Ch/SiO₂NPs) biosorbent. This biosorbent was developed to enhance the adsorption properties of the SiO₂NPs by integrating chitosan, which provides additional functional groups for effective interaction with dye molecules. The detailed characterization of this Ch/SiO₂NP biosorbent, including its structural, morphological, and chemical properties, is thoroughly discussed in *Chapter 5*, specifically at the *R & D section* under the points *5.3.1* and *5.3.2*.

Table 6.1 presents the characterization techniques and corresponding results discussed in detail earlier. The developed Ch/SiO₂NP biosorbent is directly applied for CR dye removal.

Table 6.1: Characterization techniques and their results

Properties	Pluronic mediated SiO₂NPs	Ch/SiO₂NPs	Characterization Techniques
Particles size	22.3 nm	39.8 nm	DLS
Surface charge	-42 ± 3	37 ± 2	Zeta potential
Size/Shape	18 nm/spherical	45.8 nm/spherical	TEM/FE-SEM
Nature	Amorphous	Amorphous	XRD
Surface area	1089 m ² /g	830 m ² /g	BET
Pore volume	1.38 cm ³ /g	0.83 cm ³ /g	

6.4.2: CR Dye removal

As sulfonate and azo groups attached to aromatic rings, CR is classified as the sulfonated azo dye [1]. CR dye is known for its wide applications in the cosmetics, textiles, leather, electro-optics, foodstuffs, and paper industries [2, 3]. It is highly water-soluble and quite toxic with carcinogenic properties, impacting on the eyes, skin, respiratory, and reproductive systems. Due to its complex aromatic structure, CR is highly stable, non-biodegradable, and not easily removed from water. However, Ch_{1.0}/SiO₂NPs with polycationic properties of chitosan was effectively applied for the removal of this anionic dye [4]. Analytical curve in the aqueous solutions with a known concentration of the CR dye shown in Figure 6.1.

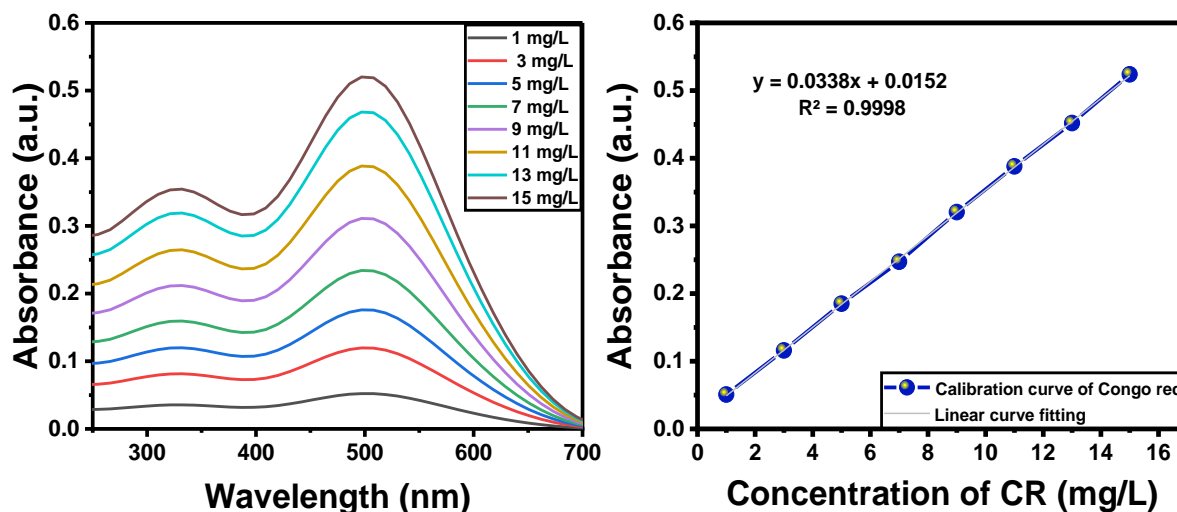


Figure 6.1: UV-Visible spectra and calibration curve of CR dye in water at RT.

The effect of biosorbent doses (25 mg to 100 mg) on the CR concentration of 200 mg/L at RT for 780 min was investigated, and results of dye removal efficacy in the form of adsorption were displayed in Figure 6.2(a). Results clearly showed the efficiency of CR removal was reached at 61.91%, 73.10%, 98.40%, 98.55%, and 98.91% for the doses 25 mg, 35 mg, 50 mg, 75 mg, and 100 mg, respectively, after the completion of 780 min. Increasing the biosorbent dose provided more surface area along with the functionality of chitosan, improving CR dye adsorption. The highest adsorption/removal was found at 50 mg, and after that there was no significant removal seen with a higher amount of biosorbent. Therefore, 50 mg was chosen as the optimal dose of $Ch_{1.0}/SiO_2NPs$ for further CR dye removal studies.

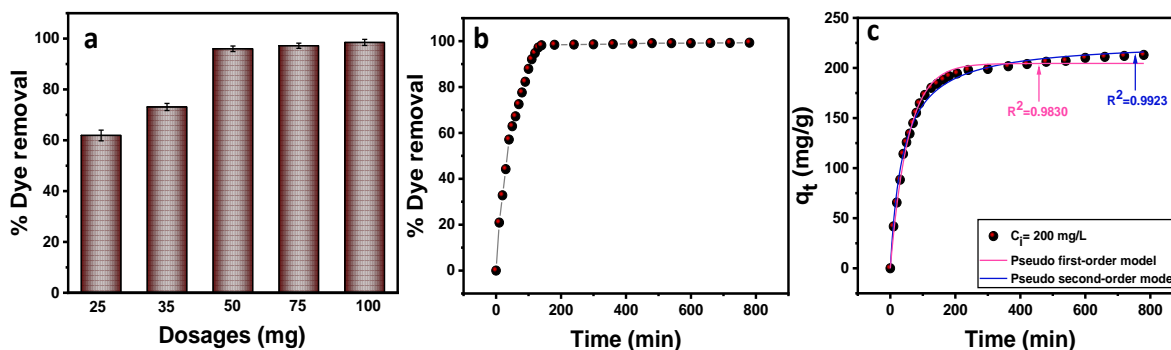


Figure 6.2. (a) CR dye removal at varying dosages, (b) the effect of time on CR dye removal, and (c) pseudo-first-order and pseudo-second-order models. ($C_i=200$ mg/L, and $M_{adsorbent}=50$ mg).

Chapter-6: Pluronic mediated silica nanoparticles with chitosan as composite for the dye removal

The time-dependent behavior of CR adsorption was investigated by changing the contact time between adsorbate (CR dye) and adsorbent (50 mg Ch_{1.0}/SiO₂NPs) ranging from 0-780 minutes. UV-Vis spectroscopy was used to measure CR dye concentration at a wavelength of $\lambda_{\text{max}} = 498$ nm, allowing for the determination of % CR dye removal with time. Figure 6.3 shows the UV-Visible spectra of CR dye absorbencies (from initial concentration, $C_i = 200$ mg/L) at different time intervals in the presence of biosorbent Ch_{1.0}/SiO₂NPs and clearly monitors the decrease in concentration of CR dye in the solution. The % CR dye removal versus contact time plot is shown in Figure 6.2(b). Results showed that the 21% dye was adsorbed in the first 10 min, which reached 67% in 50 min, and finally attained equilibrium with removal percentages of 98.40% at 130 min. CR dye adsorption is very rapid at the initial stage, and when it reaches the equilibrium stage then it is found to be very slow down and almost constant thereafter in the studied period. Such results clearly indicated that many surface sites with a large numbers of vacant pores and functional groups of Ch/SiO₂NPs are available for dye adsorption at the initial stage, but over a period of time, these surface sites become saturated, making it difficult to attach more CR dye molecules.

Whether the adsorption process done by the catalyst is controlled by physical adsorption (physisorption) or chemical adsorption (chemisorption) has been determined through the kinetic models. A pseudo-first-order model may suggest physical adsorption, while a pseudo-second-order model often indicates chemisorption [5, 6]. Results of kinetic studies for CR dye adsorption at an initial concentration of 200 mg/L at 25°C, for a period of 0 to 780 min, are shown in Figure 6.2(c). Two models (pseudo-first-order and pseudo-second-order) were successfully analyzed for the kinetics parameters. The experimental data followed the pseudo-second-order model. It clearly indicated that the adsorption process involves chemical interactions between the adsorbate (CR dye) and adsorbent (Ch_{1.0}/SiO₂NPs).

Chapter-6: Pluronic mediated silica nanoparticles with chitosan as composite for the dye removal

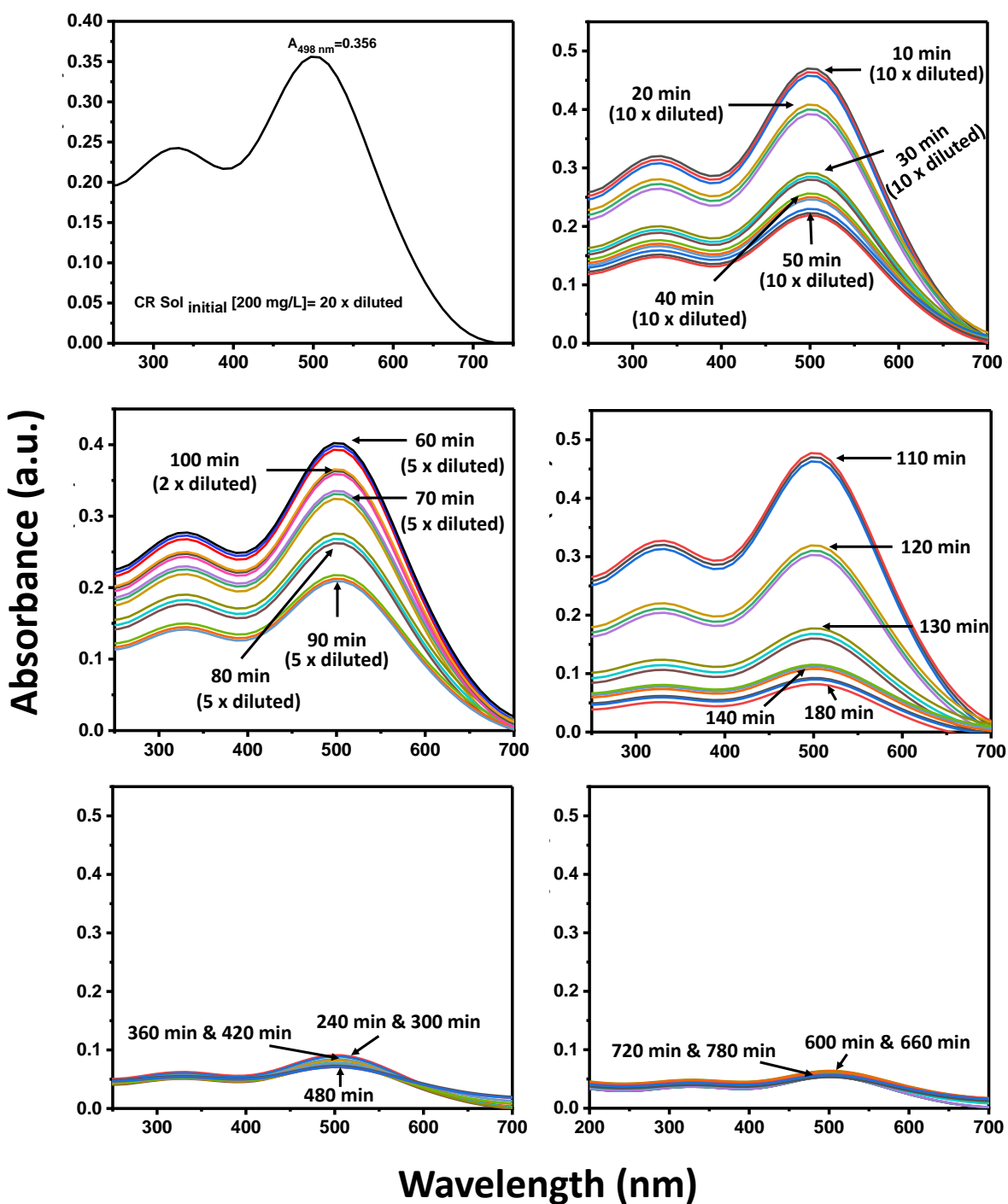


Figure 6.3: UV-visible spectrum before and after CR dye adsorption at different different time intervals. Samples are taken in triplicate.

A study of adsorption isotherms described the relationship between the amounts of adsorbate adsorbed by the adsorbent (q_e) and the concentration of the adsorbate remaining in the solution

Chapter-6: Pluronic mediated silica nanoparticles with chitosan as composite for the dye removal

after the system reaches equilibrium (c_e) at a constant temperature. In the present study, different isothermal models (Langmuir [7], Freundlich [8], and Liu models [9]) were analyzed and displayed in Figure 6.4(a). The Langmuir isotherm is based on the postulation that a monolayer of adsorbate forms at the external surface of the adsorbent and ascribes a homogeneous adsorption process. The Freundlich isotherm suggests that multilayers of adsorbate establish themselves on the external surface of the adsorbent and indicate a heterogeneous adsorption process. Also, the Liu isotherm is based on the combined characteristics of both the Langmuir and Freundlich isotherms. It offers a flexible approach to describing adsorption processes on heterogeneous surfaces. As per the results of Figure 6.4(a), the Liu isotherm model provides the best fit among the other two models in the case of CR dye removal on the surface of $\text{Ch}_{1.0}/\text{SiO}_2\text{NPs}$. Hence, it was confirmed that the multilayers of CR dye molecules adsorbed on the surface of the biosorbent $\text{Ch}_{1.0}/\text{SiO}_2\text{NPs}$.

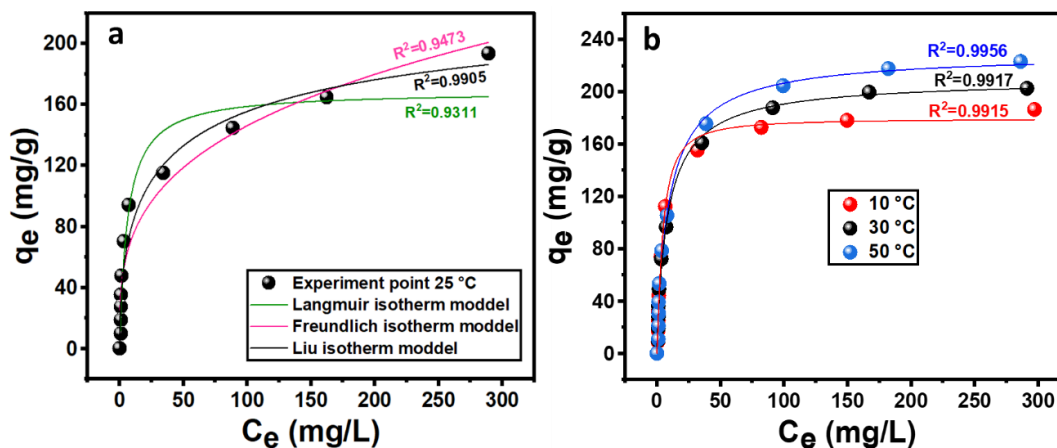


Figure 6.4: (a) Different models of isotherms plotted for experimental data obtained at 25 °C. (b) Adsorption Liu isotherms for CR adsorbed by $\text{Ch}_{1.0}/\text{SiO}_2\text{NPs}$ at 10 °C, 30 °C, and 50 °C.

In addition to examining the adsorption process of the $\text{Ch}_{1.0}/\text{SiO}_2\text{NPs}$ biosorbent for CR dye, we also studied the temperature effect on the adsorption process (Figure 6.4(b)) to understand the efficiency of the biosorbent for the removal of dye in low and high temperature environments. As per the results obtained from Figure 6.4(b), it was found that the adsorption capacity of the $\text{Ch}_{1.0}/\text{SiO}_2\text{NPs}$ increases with an increase in temperature. Here, the adsorption capacity of the biosorbent increases with temperature as an endothermic process occurs. Such adsorption rises with temperature because of enhanced the mobility of dye molecules and quite more availability of active sites at higher temperatures [10-12]. These observations are also justified by the

Chapter-6: Pluronic mediated silica nanoparticles with chitosan as composite for the dye removal

thermodynamic parameters estimated through the plot of $\ln K_L$ versus $(1/T)$ (shown in Figure 6.5). The values of thermodynamic parameters, i.e., enthalpy, entropy, and Gibbs free energy, are listed in Table 6.2. It was clearly understood that the positive value of enthalpy indicates the endothermic nature of the adsorption process, and the negative value of Gibbs free energy indicates its spontaneous nature. All the measurements proved that the $Ch_{1.0}/SiO_2NPs$ biosorbent is efficient adsorbent for the removal of CR dye at ambient temperature.

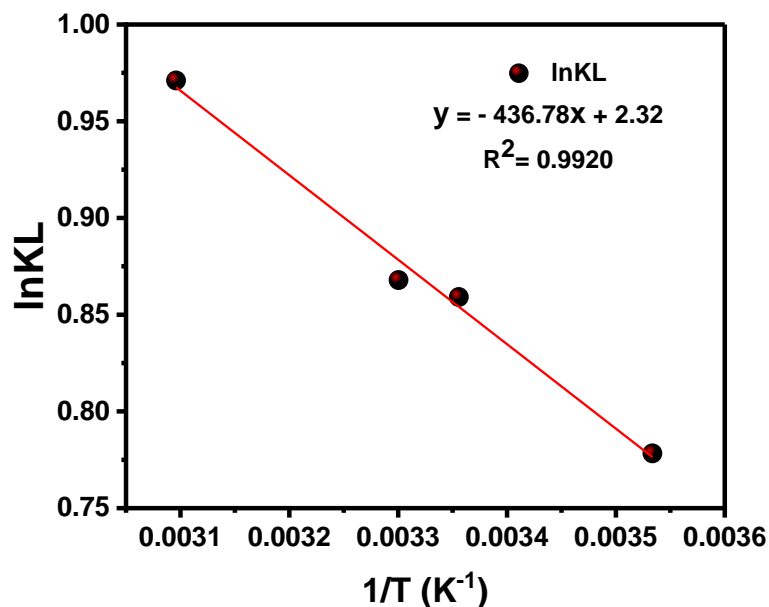


Figure 6.5: Van't Hoff plot for CR dye adsorption from aqueous solutions on the $Ch_{1.0}/SiO_2NPs$ biosorbent at 10°C, 25°C, 30°C, and 50°C (in the form of Kelvin taken in the plot).

Table 6.2: Values of thermodynamic parameters estimated for the CR dye adsorption on the $Ch_{1.0}/SiO_2NPs$ at varied temperatures (10°, 25°, 30°, and 50 °C).

Temperature	ΔG [kJ/mol]	ΔS [kJ/molK]	ΔH [kJ]	R^2
10 °C	-1.831	0.019	3.631	0.9920
25 °C	-2.128			
30 °C	-2.186			
50 °C	-2.607			

The recyclability of biosorbent $Ch_{1.0}/SiO_2NPs$ has been assessed, and their adsorption efficiency at different cycles and UV-visible spectra of the CR dye solution at use of the same $Ch_{1.0}/SiO_2NPs$ biosorbent at different cycles at RT were presented in Figure 6.6.

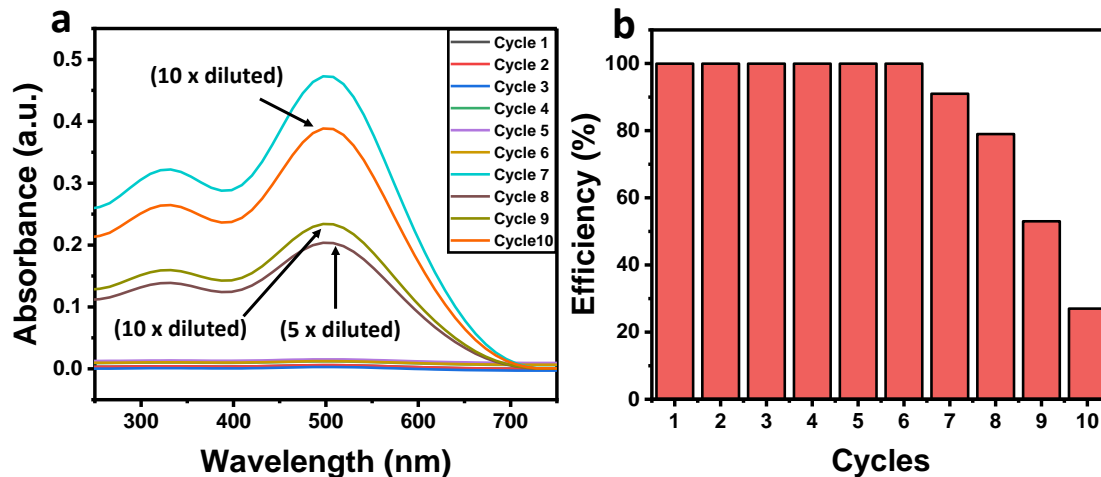


Figure 6.6: (a) Recycling of $Ch_{1.0}/SiO_2NPs$ after CR adsorption (b) UV-visible spectra of the reuse cycles of Ch/SiO_2NPs after CR adsorption, $C_i = 150$ mg/L at $25^\circ C$ for 780 min, adsorbent mass 0.5 g/L.

The adsorption efficiency of $> 95\%$ of CR dye by $Ch_{1.0}/SiO_2NPs$ has been shown up to the six cycles of the measurements. However, it was starting to decrease exponentially from the seventh cycle, with almost 26.8% efficiency remaining in the tenth cycle of $Ch_{1.0}/SiO_2NPs$ used. Here, the decline in % efficiency of biosorbent was found because of two reasons. First, in the process of adsorption, some of the chitosan molecules did not remain on the surface of mesoporous SiO_2NPs in the biosorbent, which ultimately affected the attraction of CR dye molecules for adsorption. Second, with the use of multiple times, the biosorbent surfaces change because of aggregation, which reduces the adsorption efficiency over time [13].

These promising results show that biosorbent $Ch_{1.0}/SiO_2NPs$ can be employed efficiently and affordably. The findings indicate that these biosorbents have the ability to efficiently concentrate analytes (organic molecules) at low concentrations. This provides new opportunities to apply solid phase adsorption strategies with the developed biosorbent, which can be more efficient and economically viable.

6.5: References

1. Harja, M., Buema, G. and Bucur, D., 2022. Recent advances in removal of congored dye by adsorption using an industrial waste. *Scientific reports*, 12(1), p.6087.
2. Afkhami, A. and Moosavi, R., 2010. Adsorptive removal of Congo red, a carcinogenic textile dye, from aqueous solutions by maghemite nanoparticles. *Journal of hazardous materials*, 174(1-3), pp.398-403.
3. Ghorai, S., Sarkar, A.K., Panda, A.B. and Pal, S., 2013. Effective removal of Congo red dye from aqueous solution using modified xanthan gum/silica hybrid nanocomposite as adsorbent. *Bioresource technology*, 144, pp.485-491.
4. Budnyak, T.M., Błachnio, M., Slabon, A., Jaworski, A., Tertykh, V.A., Deryło-Marczewska, A. and Marczewski, A.W., 2020. Chitosan deposited onto fumed silica surface as sustainable hybrid biosorbent for Acid Orange 8 dye capture: Effect of temperature in adsorption equilibrium and kinetics. *The Journal of Physical Chemistry C*, 124(28), pp.15312-15323.
5. Madan, S., Shaw, R., Tiwari, S. and Tiwari, S.K., 2019. Adsorption dynamics of Congo red dye removal using ZnO functionalized high silica zeolitic particles. *Applied Surface Science*, 487, pp.907-917.
6. Munagapati, V.S., Wen, H.Y., Wen, J.C., Gutha, Y., Tian, Z., Reddy, G.M. and Garcia, J.R., 2021. Anionic congo red dye removal from aqueous medium using Turkey tail (*Trametes versicolor*) fungal biomass: adsorption kinetics, isotherms, thermodynamics, reusability, and characterization. *Journal of Dispersion Science and Technology*, 42(12), pp.1785-1798.
7. Langmuir, I., 1918. The adsorption of gases on plane surfaces of glass, mica and platinum. *Journal of the American Chemical society*, 40(9), pp.1361-1403.
8. Umpleby II, R.J., Baxter, S.C., Bode, M., Berch Jr, J.K., Shah, R.N. and Shimizu, K.D., 2001. Application of the Freundlich adsorption isotherm in the characterization of molecularly imprinted polymers. *Analytica Chimica Acta*, 435(1), pp.35-42.
9. Liu, Y. and Liu, Y.J., 2008. Biosorption isotherms, kinetics and thermodynamics. *Separation and purification technology*, 61(3), pp.229-242.

Chapter-6: Pluronic mediated silica nanoparticles with chitosan as composite for the dye removal

10. Argun, M.E., Dursun, S., Ozdemir, C. and Karatas, M., 2007. Heavy metal adsorption by modified oak sawdust: Thermodynamics and kinetics. *Journal of hazardous materials*, 141(1), pp.77-85.
11. Elizalde-González, M.P. and García-Díaz, L.E., 2010. Application of a Taguchi L16 orthogonal array for optimizing the removal of Acid Orange 8 using carbon with a low specific surface area. *Chemical Engineering Journal*, 163(1-2), pp.55-61.
12. Marczewski, A.W., Seczkowska, M., Deryło-Marczewska, A. and Blachnio, M., 2016. Adsorption equilibrium and kinetics of selected phenoxyacid pesticides on activated carbon: effect of temperature. *Adsorption*, 22, pp.777-790.
13. Guan, H., Bestland, E., Zhu, C., Zhu, H., Albertsdottir, D., Hutson, J., Simmons, C.T., Ginic-Markovic, M., Tao, X. and Ellis, A.V., 2010. Variation in performance of surfactant loading and resulting nitrate removal among four selected natural zeolites. *Journal of hazardous materials*, 183(1-3), pp.616-621.